Designed interaction potentials via inverse methods for self-assembly

Mikael Rechtsman,[1] Frank Stillinger,[2] and Salvatore Torquato[2,3,*]
[1]*Department of Physics, Princeton University, Princeton, New Jersey 08544, USA*
[2]*Department of Chemistry, Princeton University, Princeton, New Jersey 08544, USA*
[3]*Program in Applied and Computational Mathematics and PRISM, Princeton, New Jersey 08544, USA*
(Received 16 September 2005; published 19 January 2006)

We formulate statistical-mechanical inverse methods in order to determine optimized interparticle interactions that spontaneously produce target many-particle configurations. Motivated by advances that give experimentalists greater and greater control over colloidal interaction potentials, we propose and discuss two computational algorithms that search for optimal potentials for self-assembly of a given target configuration. The first optimizes the potential near the ground state and the second near the melting point. We begin by applying these techniques to assembling open structures in two dimensions (square and honeycomb lattices) using only circularly symmetric pair interaction potentials; we demonstrate that the algorithms do indeed cause self-assembly of the target lattice. Our approach is distinguished from previous work in that we consider (i) lattice sums, (ii) mechanical stability (phonon spectra), and (iii) annealed Monte Carlo simulations. We also devise circularly symmetric potentials that yield chainlike structures as well as systems of clusters.

DOI: 10.1103/PhysRevE.73.011406 PACS number(s): 82.70.Dd, 81.16.Dn

I. INTRODUCTION

"Self-assembly" of atomic, molecular, and supramolecular systems is a topic that has been receiving a great deal of attention of late. Roughly speaking, it is the phenomenon of system components arranging themselves via their mutual interaction to form a larger functional unit. Examples are plentiful; in biology, they include but are not limited to the spontaneous formation of the DNA double helix from two complementary oligonucleotide chains, the formation of lipid bilayers as membranes, and spontaneous protein folding into the native, functional state. On the other hand, self-assembly can be employed in the synthesis of nanostructures as an alternative to nanolithography. For example, Whitesides [1] has demonstrated that complex two-dimensional structure can emerge in organic molecules placed on an inorganic surface. This is a natural system for studying self-assembly in two dimensions. Jenekhe and Chen [2] showed self-assembly of block copolymers into ordered arrays for possible use as photonic band-gap materials. Block copolymers are indeed natural candidates for use in photonic devices due to the elaborate structures they can form and their multiple dielectric constants. Stellacci *et al.* [3] have shown how gold nanowires can be assembled by functionalizing nanoparticles with organic molecules. Manoharan *et al.* [4] have demonstrated extremely robust self-assembly of unique, small clusters of microspheres that can themselves be used for self-assembly of more complex architectures.

This is an emerging field with a wealth of experimental data that does not yet have a predictive theoretical basis. Where there has been theoretical work, it has focused on explaining the self-assembly in systems with given interparticle interactions [5,6] or of known macromolecular structure [6]. These studies solve the "forward" problem of statistical mechanics, i.e., they take the interaction as known and solve for the structure and equilibrium properties of the system. In this study, we take the inverse appraoch—given a desired many-particle configuration of the system, we search for the optimal interaction among component particles which spontaneously produces that target structure.

Our goal is to introduce an inverse statistical-mechanical methodology for optimizing adjustable interactions for targeted self-assembly. Motivation for this comes from the plethora of recent examples wherein materials have been designed to possess predetermined properties. Examples of these include novel crystal structures for photonic band-gap applications [7], materials with negative or vanishing thermal expansion coefficients [8,9], materials with negative Poisson ratios [10], materials with optimal transport and mechanical properties [11], mesoporous solids for applications in catalysis, separations, sensors and electronics [12,13], and systems characterized by entropically driven inverse freezing [14]. Our goal is to devise methods that can be applied to any predetermined target structure, be they amorphous or even quasicrystalline, thus extending the traditional meaning of self-assembly beyond that of periodic structures.

We choose colloidal systems [15] as models for studying self-assembly. Colloids are ideally suited for this purpose because interparticle interactions are tunable. The colloid interparticle potential $V(r)$ can contain a hard-core term, a charge dispersion (van der Waals) term, a dipole-dipole term [isotropic in two dimensions (2D)], a screened-Coulombic (Yukawa) term, and a short-ranged attractive depletion term. All of these have adjustable amplitudes, and in the case of the Yukawa term, the screening length can be adjusted by changing the salt concentration in solution. Taken together, these interactions form a large set of functional forms for the interaction potential. Although we do not limit ourselves in this study to these interactions, we bear in mind the limits of complexity that these interactions will allow and we try not to exceed these bounds in searching for our optimized potentials.

*Corresponding author. Email address: torquato@princeton.edu

The adjustable colloidal interactions discussed in the previous paragraph are by nature isotropic. Thus, in this study, we consider only potentials that have this property. Even for this relatively simple class of potentials it is not at all clear what are the limitations for self-assembly. For example, chiral structures with specified handedness cannot be distinguished energetically from their mirror-image counterpart. What other structures cannot be valid target structures? A central question in colloidal and photonics research is regarding whether a diamond lattice (in three dimensions) can be self-assembled, since such a lattice of dielectric spheres has a large photonic band gap and would therefore be a viable material for future photonic devices. It is not known whether a diamond lattice can be assembled using isotropic colloidal particles; indeed, the bonding in diamond itself is highly directional.

There has been recent interest in self-assembly of anisotropic particles. Examples of these are the so-called "patchy particles" [16] and the unique colloidal clusters of Manoharan *et al.* discussed above, which are anisotropic simply by virtue of their nonspherical shapes. Although our algorithms can be easily generalized to nonisotropic interactions, we restrict ourselves to studying self-assembly with isotropic potentials since this *per se* is a complex and subtle problem, and a very nontrivial test bed for our optimization schemes. Also, isotropic colloids are easy to produce by comparison and their potential forms are manipulated relatively easily.

A general potential energy function for a system of classically interacting particles at positions $\{\mathbf{r}_i\}$ in zero external field can be written as

$$\Phi(\{\mathbf{r}\}) = \sum_{i<j} V_2(\mathbf{r}_i, \mathbf{r}_j) + \sum_{i<j<k} V_3(\mathbf{r}_i, \mathbf{r}_j, \mathbf{r}_k) + \cdots, \qquad (1)$$

where the V_β's are β-body potentials. Since we only consider systems with isotropic interactions, we write

$$\Phi(\{\mathbf{r}\}) = \sum_{i<j} V(|\mathbf{r}_i - \mathbf{r}_j|). \qquad (2)$$

Two necessary conditions that a pair potential correspond to a targeted ground-state lattice are that (i) it is energetically favored among a host of other lattices over a significant specific area α range (stable lattice sums) and (ii) possesses real phonon frequencies at every wave vector in the Brillouin zone (stable phonons).

Past work on lattice self-assembly has not used both energy and mechanical stability criteria in tandem as we do here; we consider this to be a main strength of our approach. Still, these conditions are not universally sufficient for any pair interaction and lattice structure. However, taken together, these necessary conditions constitute a prescription for finding pair potentials that most robustly stabilize a given target lattice. In the first optimization scheme (both are described further on), a pair potential is found that maximizes the energy gap between the target lattices and its competitors, while keeping all phonon frequencies real. The second scheme assumes stable lattice sums and real phonon frequencies, and uses molecular dynamics (MD) simulations to maximize the stability of the lattice near its melting point.

For the purposes of this study, we will say that a lattice is self-assembled if it is formed from a random configuration in a well equilibrated, annealed Monte Carlo (MC) simulation in an *NVT* ensemble, where N is the number of particles, V is the volume of the system, and T is the absolute temperature. It should be emphasized that the requirement that a given lattice self-assemble in a MC simulation is a very strong one. In conventional theoretical studies of colloidal crystallization [17], a number of candidate lattices is chosen and a phase diagram is drawn by comparing free energies of the lattices to each other and the liquid state over a range of thermodynamic parameters. However, this procedure says nothing of mechanical stability, or whether crystallization of the lattice is preempted by that of another structure not considered. These shortcomings are removed when self-assembly in an MC, from a random initial configuration, is required. That said, finite-size effects and limited CPU time in an MC simulation might prevent self-assembly of a structure that should form.

In the present paper we specialize to target structures that are two dimensional. In particular we seek optimal potentials for self-assembly of the square and honeycomb lattices, the latter being the two-dimensional analog of the diamond lattice (four maximally separated neighbors in 3D versus three maximally separated neighbors in 2D). This would be the first demonstration of which we are aware of a lattice as sparse as the honeycomb being self-assembled in an annealed MC simulation. This work is an expansion on a previous introductory note by the present authors [18]. In this paper, an optimization algorithm is introduced and applied. In addition to the honeycomb lattice considered in the previous work, the triangular (as a control) and square lattices are studied. We make the case for a more stringent requirement for self-assembly and investigate the use of linear-ramp potentials for this purpose. A more extensive discussion of the problem of self-assembly in systems with isotropic interactions is given in the conclusion section, including some MC results for colloidal clusters and colloidal chains. In a future paper, we will apply these inverse methods to three-dimensional colloidal systems. While it is certainly true that many-body behavior is fundamentally different in 3D, our methods are easily generalizable to higher dimensions, and we believe they will be as effective.

In the following section, we discuss past work on this topic both for the sake of motivation and to show work upon which we have attempted to improve. This is followed by a section describing our optimization schemes. Next are sections on the triangular, square and honeycomb lattices, with potentials for their self-assembly and details of their applications. We discuss the triangular lattice here as a control case, and to give the details of our simulation procedure. The final section is the discussion of our results and some conclusions based on them.

II. PREVIOUS WORK

Weber and Stillinger [19] examined self-assembly of a square lattice for a particular potential that included two- and three-body interactions. They found that for their potential,

the square lattice was indeed the ground state and demonstrated that it self-assembled in a 2500 particle molecular dynamics simulation. Our work is motivated by this, but is different in two key ways. The first is that we restrict ourselves to a much smaller class of potential functions, namely, those that are two body only and isotropic. This should make our potentials lend themselves better to realization in the lab. The second is that we are searching systematically for functional forms for $V(r)$ that stabilize open structures, whereas in Ref. [19], the authors postulated a potential that seemed that it should favor the square lattice and studied its properties. Weber and Stillinger took the direct approach, we take the inverse approach.

The so-called "reverse" Monte Carlo method [20] of Lyubartsev *et al.* was devised to find interparticle potentials that produced given liquid state pair correlation functions. A similar method was developed by Muller-Plathe [21] using simplex optimization. Although these are inverse techniques, they are fundamentally different from our methods here for two reasons. The first reason is that the pair correlation function contains limited information about an N-particle configuration. Our method produces assembly of a given configuration. The second reason is that these techniques fundamentally deal with liquids and so do not apply to self-assembly as it is commonly defined.

Jagla claims in Ref. [5] to have found an isotropic pair potential form that stabilizes a number of structures (including a "distorted" honeycomb lattice) called the "linear-ramp" potential, which consists of a hard core at $r=1$ plus a linear tail going to zero at a distance $r_1>1$. A phase diagram is drawn in that paper indicating the stability of the structures he lists for different pressures and values of r_1. However, he never actually carried out a stability analysis and therefore it is questionable whether the structures in his phase diagram are truly ground states. Motivated by this issue, we determine whether the square lattice can be assembled over a nontrivial specific area range for such a simple potential and choose $r_1=1.45$, which the phase diagram indicates should yield the square lattice for certain pressure values. For this value of r_1 we find the range in specific area α for which the square beats out the other three lattices (see Fig. 1), and find the phonon spectra (see Fig. 2) over that range. Phonon spectra were calculated in the standard way by diagonalizing the dynamical matrix for a very fine grid of k points in the Brillouin zone (a detailed explanation of this is given in Ref. [22]). Any lattice at a given specific area/volume that has an imaginary phonon frequency at any wave vector is necessarily mechanically unstable. An NVT MC simulation of 625 particles annealed from $k_BT=1.5$ to $k_BT=0.05$ is shown at $\alpha=1.38$ in Fig. 3. Although there are pockets of square lattice present, it is clear that the lattice has not assembled, and there is no long range order. This can be seen from the plot of the structure factor $S(\mathbf{k})$, given in Fig. 4. One of two things has happened here. Either the system has become a glass, or it has no freezing transition. This suggests that comparing the energies of a number of lattices (as was done in Ref. [5]) cannot alone give certainty of the ground state.

III. THE OPTIMIZATION SCHEMES

A central feature of our approach to the inverse problem is the design of computational algorithms that search for and optimize a functional form for $V(r)$ that leads to self-assembly of a given target structure. The direct (noninverse) version of this is the problem of the first order freezing transition, and has been studied analytically and numerically using, for example, classical density functional methods [23].

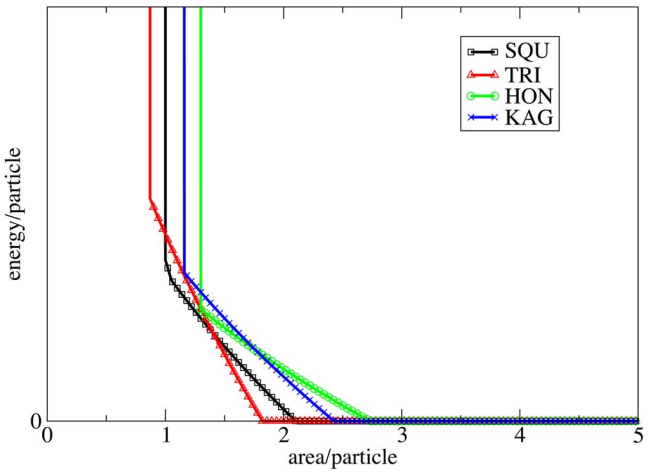

FIG. 1. (Color online) Lattice sums for the linear-ramp potential with $r_1=1.45$. Square wins out for values of the specific area α between 1 and 1.4.

Optimizing a pair potential $V(r)$ for self-assembly means choosing a family of functions $V(r;\{a_0\cdots a_n\})$, parametrized by the a_i's, and then finding the values of the parameters that lead to the most robust and defect-free self-assembly of the target lattice, at a given specific volume α (or specific area in 2D). We must be careful to choose the parameters such that an overall rescaling of the potential is not possible, and we keep each parameter within a prespecified range $[a_i^{\min},a_i^{\max}]$. The choice of parametrization and initial parameter values is important: we make educated guesses based on the coordination numbers of lattices close in structure to the target

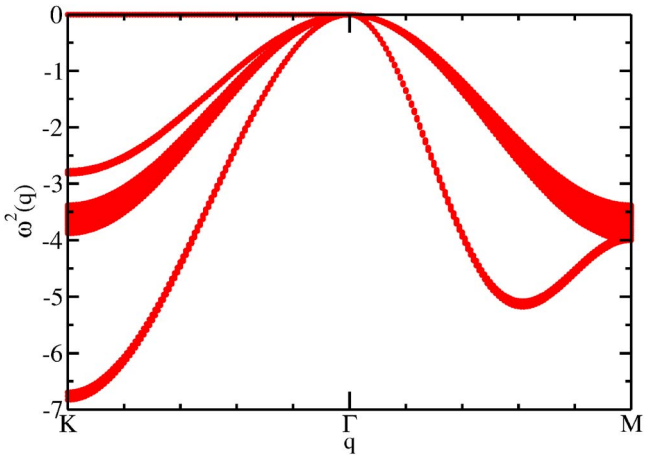

FIG. 2. (Color online) Phonon spectra for specific area $\alpha=1.0$ to $\alpha=1.4$ for the square lattice in the linear ramp potential with $r_1=1.45$. Bands form as a result of the variation in α. Over this entire range of α, all frequencies are imaginary, which indicates mechanical instability in the lattice. Over this density range, the square lattice is clearly not the ground state.

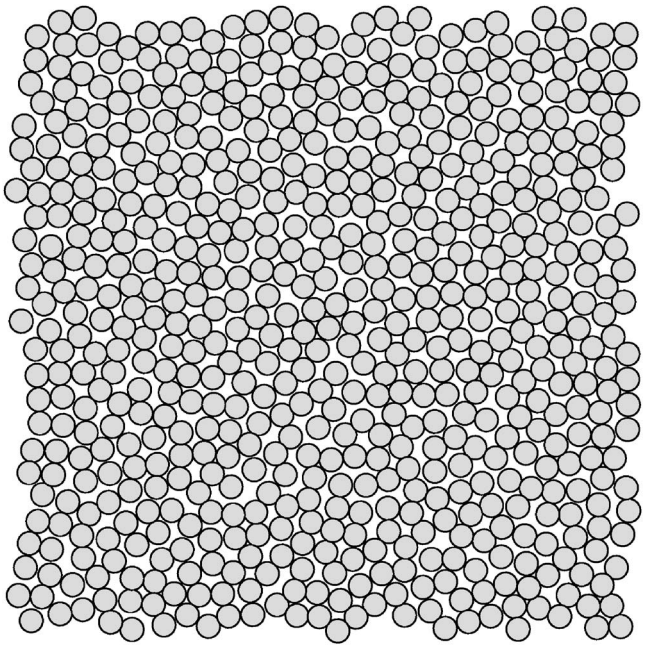

FIG. 3. 625-particle MC results for the linear-ramp potential. Annealed from $k_BT=1.1$ to $k_BT=0.02$ at $\alpha=1.38$.

lattice. Optimization can be carried out either at zero temperature or near melting.

A. $T=0$ optimization scheme

Once the parametrization and initial parameters are chosen, we perform a simulated annealing optimization to maximize the difference in lattice energy per particle ϵ between the target lattice and its closest energetic competitor among the principle lattices in the system dimension (e.g., in 2D, among triangular, square, honeycomb, and Kagomé lattices). This procedure is called the "zero-temperature" scheme because it seeks to minimize the difference in lattice potential energies, rather than free energies; it is a search for stable ground states. Formally, if $\epsilon(\alpha)$ is the energy per particle at specific volume α, we take as our objective function

$$\Theta_1 = \max_j \left[\min_{\alpha\in[\alpha_{\min},\alpha_{\max}]} \epsilon^T(\alpha) - \min_{\alpha\in[\alpha_{\min},\alpha_{\max}]} \epsilon^j(\alpha) \right]. \quad (3)$$

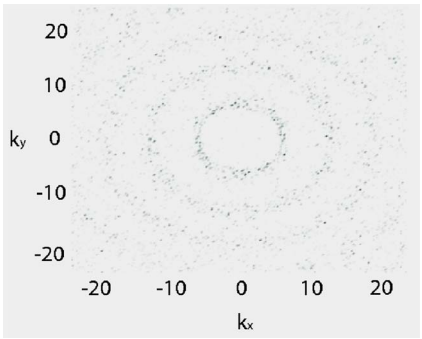

FIG. 4. (Color online) The structure factor $S(\mathbf{k})$ for configuration in Fig. 3, where k_x and k_y are the Cartesian components of the wave vector $\mathbf{k}$. This pattern in $S(\mathbf{k})$ indicates that there is no long-range order in this configuration.

Here, T refers to the target lattice, j enumerates the competitor lattices and $[\alpha_{\min},\alpha_{\max}]$ is a specific volume range, within which the target α lies. The simulated annealing is performed in a_i parameter space, searching for a potential that minimizes Θ_1. This alone is not sufficient; we must also guarantee the mechanical stability of the lattice. This is done by making sure that at the target α, the given potential is such that every phonon mode in the Brillouin zone is real. In practice, this is done by constraining the lowest eigenvalue of the dynamical matrix (frequency squared) to be positive, and the lowest curvature eigenvalue of the softest acoustic phonon mode to be greater than some positive cutoff value. While this does not necessarily imply that all frequencies will be real, it is usually sufficient, and in any case the frequency of every mode can be calculated post facto.

In this scheme, we make the assumption that the greater the difference in lattice energy per particle ϵ (over a range of α's around the target α) of the target lattice and its principle competitors, the greater will be the target's tendency to assemble. While this is not by any means a rigorous statement, it seems to make intuitive sense—the greater the energy difference, the less the tendency to get frustrated at the freezing point between two lattices; the annealing should find the deeper energy minimum.

It is possible that another structure will preempt the target lattice (freeze at a higher temperature), even if the optimization proceeds perfectly. The MC will then get "stuck"; the simulation will never go to its ground state because it is caught in a strongly metastable state. Presumeably, however, a colloidal system with the same interaction potential would undergo a structural phase transition to the its ground state as the temperature was lowered. Our MC simulations did indeed get stuck in slightly defected configurations very close to the desired lattice. To check that these structures were not inherently more stable than the target, we always confirmed that the defects caused the system to have higher energy than that of the lattice.

The main disadvantage of this optimization procedure is that it is very specific to simple lattices, and is not naturally generalized to more complicated structures. Indeed, the CPU time required for the optimization grows as the cube of the number of basis elements in the lattice, so optimizing for complex structures quickly becomes intractable. Nonperiodic structures (e.g., quasicrystals) are thus impossible for this scheme.

This optimization scheme is competitor based; we favor the target by energetically disfavoring other lattices. However, this does not preclude other structures, periodic or otherwise from being lower in energy than the target. This is an inherent limitation of this technique. The next scheme, however, does not suffer this shortcoming.

B. "Near melting" optimization scheme

In this procedure, we first make sure that the initial potential satisfies our two stated necessary conditions for self-assembly with the initial parameter values, namely, that the target lattice is energetically favored over the others over a wide α range, and that at our chosen α, all phonon modes are

real. We then feed this family of functions to the algorithm, and optimize it for self-assembly at a temperature near (but below) the lattice's melting point by suppressing nucleation of the liquid phase in MD simulations.

We first find the melting temperature of the system by running an *NVE* (canonical ensemble) molecular dynamics simulation (MD) on a system of particles, in the target configuration, at incrementally increasing temperatures (mean square velocity). We then run the MD repeatedly at 80–95 % of the melting temperature (the temperature is chosen such that phase-transition fluctuations do not render the calculations inconsistent), each time calculating the Lindemann parameter, defined by

$$\Theta_2 = \sqrt{\frac{1}{N}\sum_i (\mathbf{r}_i - \mathbf{r}_i^{(0)})^2 - \left(\frac{1}{N}\sum_i (\mathbf{r}_i - \mathbf{r}_i^{(0)})\right)^2}, \qquad (4)$$

where $\mathbf{r}_i$ is the position of the ith particle after an appropriate amount of simulation time, $\mathbf{r}_i^{(0)}$ is its initial position, and N is the number of particles. Θ_2 is then taken as the objective function for a simulated annealing calculation, and those parameters, a_i, are found such that Θ_2 is minimized. It should be noted that in order to get a reproducible value of Θ_2, it must be averaged over a number of MD runs.

We choose to minimize the Lindemann parameter because it gives some quantitative measure of the degree of liquid nucleation or structural phase transition setting in near the melting point. Presumeably, the more these effects are suppressed, the more robustly the potential favors the given target structure. The algorithm will by its nature disfavor potentials that violate either of our two necessary conditions for self-assembly. It is inevitable that over the course of the optimization the melting temperature of the potential will be changed; it could be that at that point, the system will no longer be near the phase coexistence regime. This can be detected easily enough (for example by comparing the Lindemann parameter to that which the harmonic approximation predicts), and then the optimization can be stopped and restarted at a higher, appropriately chosen temperature.

An important limitation of this optimization is in the tradeoff between its consistency and its closeness in temperature to the melting point. Due to large fluctuations near melting, getting reproducible values for Θ_2 with sufficiently small error requires larger and larger system sizes. So while the optimization can be carried out well into the anharmonic regime, the optimization cannot sample true phase coexistence, only nucleation.

The inherent bias in this scheme towards the target lattice presents a problem for optimization. The procedure does not distinguish between a configuration being in a thermodynamically stable state at the given temperature and being in a supercooled metastable state. Just as in a MC simulation, the MD may get "stuck." As a result, the target may become strongly metastable but never thermodynamically favored. The only way to decrease this effect is to get closer in temperature to the melting point, but this in turn requires more and more CPU time.

In addition to the obvious advantage that this scheme incorporates finite-temperature, anharmonic effects, it has the advantage of being competitor free. Whereas in the $T=0$ scheme, competitor lattices have to be chosen against which the target lattice competes, this procedure ostensibly optimizes against *all* competition. It should be noted that if an initial potential with favorable lattice sums and stable phonons for this procedure cannot be found by trial-and-error, the zero-temperature scheme can be run first on a given functional parametrization. This procedure would then take that output as its input. This is perhaps the best way to combine the two optimizations.

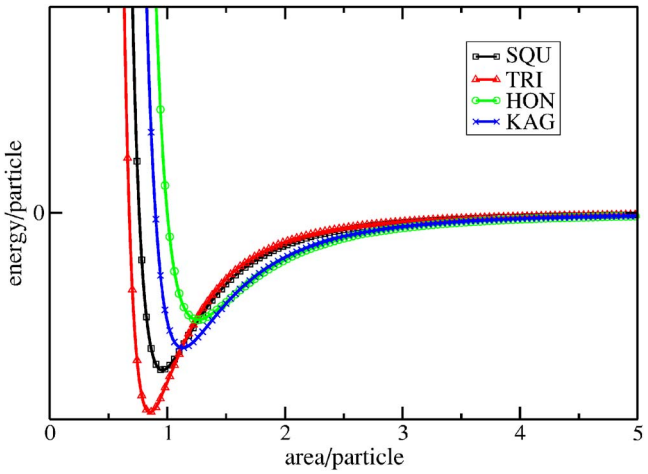

FIG. 5. (Color online) Lattice sums for the Lennard-Jones potential. The triangular lattice is the most stable structure (at positive pressure) for values of α from 0 through $\sqrt{3}/2$.

IV. THE TRIANGULAR LATTICE

A very well studied interparticle potential that robustly stabilizes the triangular lattice is the Lennard-Jones (LJ) [24], given in a form rescaled from its traditional definition

$$V(r) = \frac{1}{r^{12}} - \frac{2}{r^6}.$$

We discuss this potential here as a control. We have employed it in a 500-particle MC simulation in the *NVT* ensemble, annealing it down from $k_BT=1.5$ to $k_BT=0.2$ (allowing sufficient equilibration time at each temperature step), with specific area given by the triangular lattice area when the nearest neighbor is at unity, namely, $\sqrt{3}/2$. Lattice sums, shown in Fig. 5, demonstrate that energetically, the triangular does beat the square, honeycomb, and Kagomé lattices over a wide range of α's (actually globally in this case). Figure 6 shows that all phonon frequencies are indeed real. The two branches of course represent the longitudal and transverse acoustic modes of oscillation. Clearly the LJ potential meets our two necessary conditions, that it be energetically favored over the other lattices and that it have real phonon frequencies. Figure 7 shows that it does indeed self-assemble into the triangular lattice. The structure factor $S(k)$ shown in Fig. 8 shows conclusively the existence of long-range order here. For a different target lattice, we would have defined a family of potentials of which the LJ was one, run the optimization

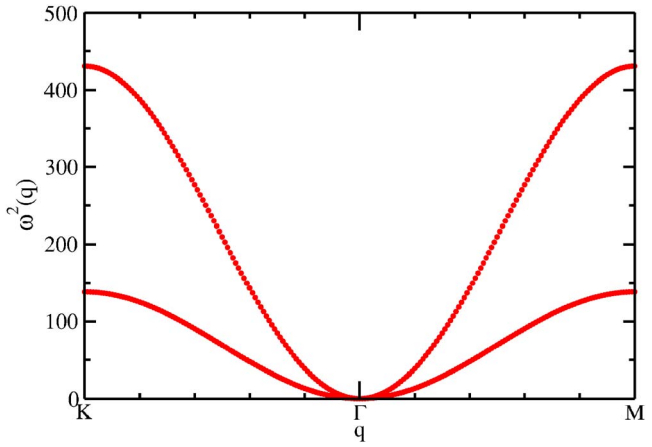

FIG. 6. (Color online) Phonon spectrum (frequency squared) for triangular lattice for the Lennard-Jones potential at $\alpha=\sqrt{3}/2$. As expected, the phonon frequencies are all real, which means that the triangular lattice is mechanically stable for this value of α.

program, and then performed the MC self-assembly calculation. We do not run the optimization for the LJ here because it is a relatively simple potential, and we wish to use it simply as a reference. Note that for all MC simulations in this study we use an *NVT* ensemble with periodic boundary conditions, adjusting the MC maximum step fraction such that 30% acceptance is maintained throughout the simulation (for maximal ergodicity) [25], and anneal through the freezing transition towards $T=0$.

V. THE SQUARE LATTICE

Finding a stabilizing potential for the square lattice is in some sense a more straightforward task than for the honeycomb lattice since the neighbor distances are different from those of the triangular. Quandt and Teter accidentally came across a pair interaction that stabilized the square lattice when examining quasiperiodic structures in 2D systems [26]. Qualitatively very similar to the optimal $V(r)$ that we derive below, their square lattice potential satisfies our necessary conditions, as expected. Their potential gives a very soft phonon branch, causing the crystal to be very sensitive to perturbations—the potential we derive below improves on this. Here we use the square lattice as a simple illustration and a test case of our methods. In finding an initial potential, we choose to start with the LJ potential. Consider an α for which the nearest neighbor distance is unity (for the square lattice, this is itself unity, i.e., $\alpha=1$), then for the triangular lattice, the next-nearest neighbor is at $r=\sqrt{3}$ and for the square lattice it is at $r=\sqrt{2}$. Thus, we desire to find a potential that is positive at $r=\sqrt{3}$ but negative at $r=\sqrt{2}$. Consider a LJ potential with an added Gaussian centered at $\sqrt{3}$ which has a low enough width so that $V(\sqrt{2})$ is negative, and has a great enough amplitude so that $V(\sqrt{3})$ is positive. This would do the job of favoring the square lattice second neighbor while excluding the triangular lattice one. Still, the amplitude and width must be chosen such that our necessary stability conditions are met. The trade-off here is clear: with an amplitude too low, the square lattice will not be energetically favored, and with an amplitude too high, the lattice will not be mechanically stable (the phonon frequencies will not be everywhere real). We have found such a potential, namely,

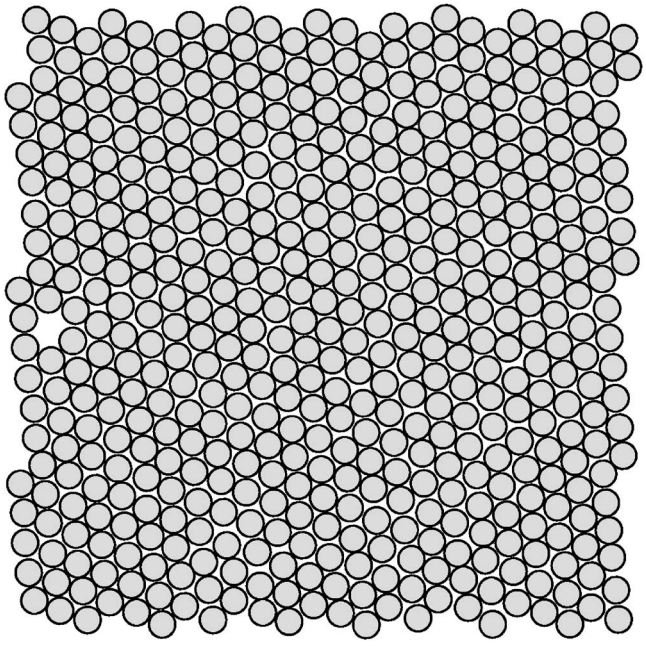

FIG. 7. 500-particle MC results for the LJ potential annealed from $k_BT=1.5$ to $k_BT=0.2$ at $\alpha=\sqrt{3}/2$.

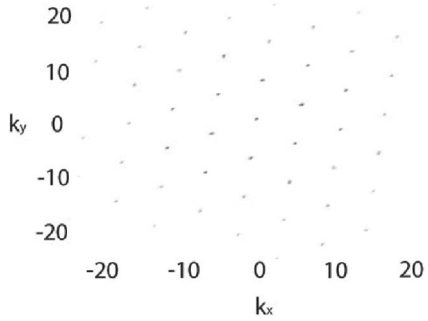

FIG. 8. $S(\mathbf{k})$ for the configuration shown in Fig. 7. The Bragg spots shown here in $S(\mathbf{k})$ clearly indicate the presence of long-range order in the LJ-annealed configuration of Fig. 7, as expected.

$$V_{\mathrm{SQU}}(r)=\frac{1}{r^{12}}-\frac{2}{r^{6}}+0.7\exp[-25(r-\sqrt{3})^2]. \qquad (5)$$

This potential is plotted in Fig. 9. The lattice sums for $V_{\mathrm{SQU}}(r)$ are given in Fig. 10 and its phonon spectrum is shown in Fig. 11. Clearly the square lattice is energetically favored and mechanically stable. The Maxwell double tangent construction applied to the lattice sums gives a range of stability in pressure (equal to $-\partial\epsilon/\partial\alpha$ at $T=0$) of 0 through 23.3, and in specific area of approximately 0.85 through 1.0.

We wish to optimize this initial guess potential and optimize it, and so we parametrize it as follows:

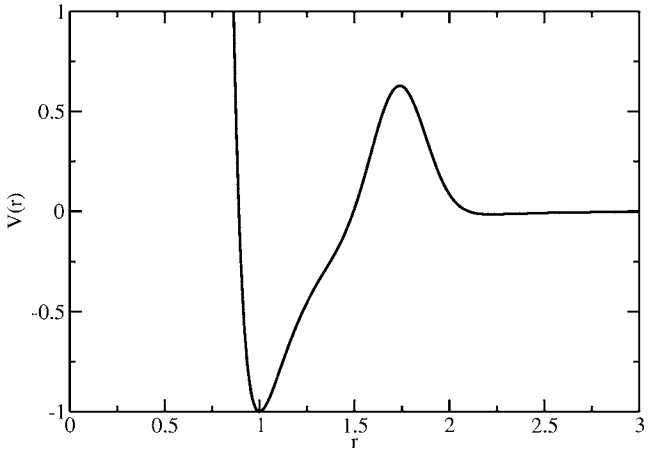

FIG. 9. A stable square-lattice potential V_{SQU}, as specified by Eq. (5). This was the initial potential given to the optimization schemes. The near-melting scheme produced the potential given in Eq. (7), and the zero-temperature scheme produced the potential given in Eq. (8).

$$V_{\mathrm{SQU}}(r;a_0,a_1,a_2) = \frac{1}{r^{12}} - \frac{2}{r^6} + a_0 \exp[-a_1(r-a_2)^2]. \quad (6)$$

Within the optimization program, we choose bounds for the parameters, somewhat arbitrarily (such that the final potential still resembles the initial guess). We ran the near-melting and the zero-temperature optimization schemes. The near-melting optimization produced the potential

$$V_{\mathrm{SQU}}(r) = \frac{1}{r^{12}} - \frac{2}{r^6} + 0.828 \exp[-26.5(r-1.79)^2], \quad (7)$$

and the zero-temperature optimization produced

$$V_{\mathrm{SQU}}(r) = \frac{1}{r^{12}} - \frac{2}{r^6} + 0.672 \exp[-42.242(r-1.8248)^2]. \quad (8)$$

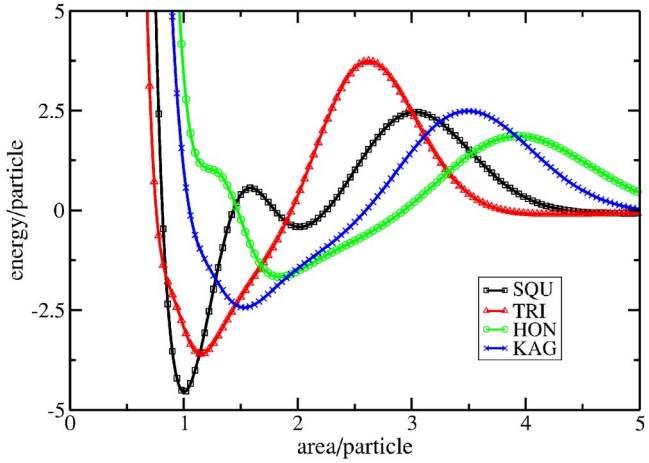

FIG. 10. (Color online) Lattice sums for the optimized square-lattice potential V_{SQU}, as specified by Eq. (7). The square lattice is the most stable structure (at positive pressure) for values of α between 0.85 and 1.0.

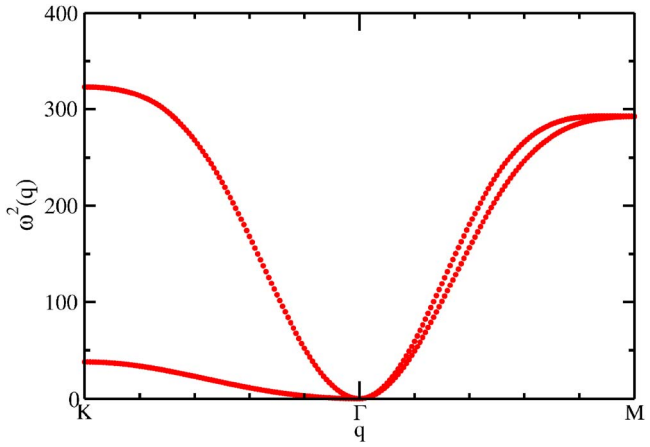

FIG. 11. (Color online) Phonon spectrum (frequency squared) of the square lattice for the optimized V_{SQU} given in Eq. (7) at $\alpha = 1.0$. This implies mechanical stability of the square lattice at this value of α.

The square lattice potentials are run in 484-particle MC calculations, annealed to $k_BT=0$ from $k_BT=1.0$, at $\alpha=1.0$. We find that the potentials from both optimization schemes cause square lattice self-assembly, as is evidenced in Fig. 12 (the MC results), and in Fig. 13, the structure factor, which shows the presence of long-range order. The results shown are for the near-melting optimization, but we obtained essentially the same results for the zero-temperature optimization. Thus, we have "solved" the inverse problem for the case of the square lattice, or at least we have found two working solutions.

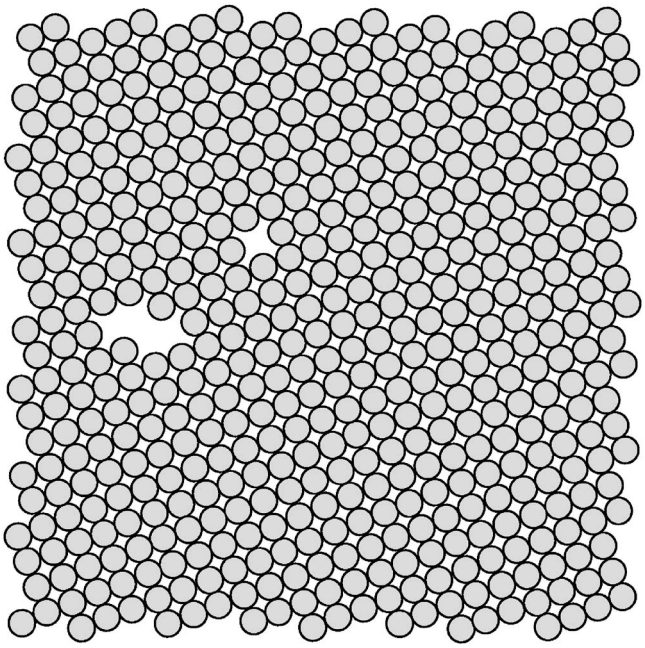

FIG. 12. 484-particle MC results for the near-melting optimized square-lattice potential V_{SQU}, as specified by Eq. (7), annealed from $k_BT=1.0$ to $k_BT=0.0$ at $\alpha=1.0$.

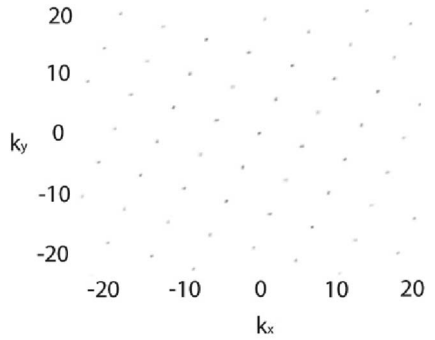

FIG. 13. $S(\mathbf{k})$ for configuration given in Fig. 12. The Bragg spots shown here in $S(\mathbf{k})$ clearly indicate the presence of long-range order in the configuration shown in Fig. 12.

VI. THE HONEYCOMB LATTICE

We base our choice for the parametrization of the honeycomb pair potential on the fact that the honeycomb is a sublattice of the triangular, sharing the same neighbor distances. The first and second coordination numbers are (3,6) and (6,6) for the honeycomb and triangular lattices, respectively. We therefore choose a potential that is positive at what we intend to be the nearest-neighbor distance. For the sake of mechanical stability (real phonon frequencies), we put a potential "well" at that distance, in the form of a 12-10 Lennard-Jones potential. Including an exponential repulsive term, we first parametrize the potential as follows:

$$V_{\mathrm{HON}}(r;a_1,a_2) = \frac{5}{r^{12}} - \frac{6}{r^{10}} + a_1 \exp[-a_2 r].$$

Phonon frequencies could not all be made real using this parametrization, and thus it was deemed to be insufficient. As a result, we add to the parametrization an attractive Gaussian of set depth and variance, meant to "brace" the second neighbor:

$$V_{\mathrm{HON}}(r;a_0,a_1,a_2,a_3) = \frac{5}{r^{12}} - \frac{a_0}{r^{10}} + a_1 \exp[-a_2 r] - 0.4 \exp[-40(r-a_3)^2]. \quad (9)$$

Note that here we are now allowing the coefficient of the $1/r^{10}$ term to vary in the optimization. After some encouraging phonon spectra, lattice sums and annealing results with a number of different parameter value inputs, we concluded that this was a sufficiently (but not overly) complex functional form on which to perform the optimization. The targeted specific area is $\alpha = 1.45$.

The initial values for the parameters were chosen to be $a_0 = 6.5$, $a_1 = 18.5$, $a_2 = 2.45$, and $a_3 = 1.83$. For comparison to optimized results, a 500-particle annealed MC simulation was run using these parameters, the result of which is shown in Fig. 14. It clearly nowhere resembles a honeycomb lattice configuration.

Both optimization schemes were carried out on this parametrization of the potential. Here, we show all results for the near-melting scheme and simply state the results for the zero-temperature scheme. The near-melting algorithm produced the following potential:

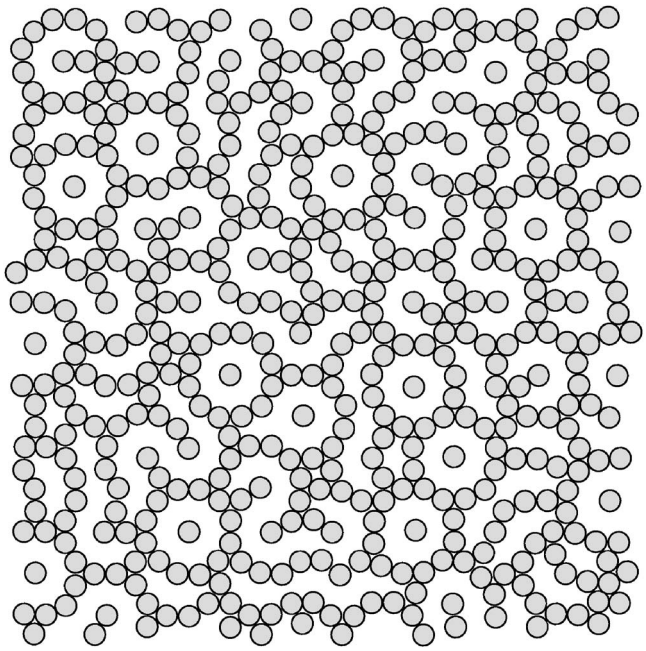

FIG. 14. 500-particle annealed MC results, for potential with parameters displaced from initial guess at $\alpha = 1.45$. This potential clearly yields a structure drastically different from the honeycomb lattice.

$$V_{\mathrm{HON}}(r) = \frac{5}{r^{12}} - \frac{5.89}{r^{10}} + 17.9 \exp[-2.49r] - 0.4 \exp[-40(r - 1.823)^2]. \quad (10)$$

This function is plotted in Fig. 15. The lattice sums and phonon spectrum are given in Figs. 16 and 17, respectively. Notice that in the region of stability of the honeycomb lattice the pressure would have to be positive in order to ensure thermodynamic stability. The reader should note, however, that in principle, it is always possible to append to a con-

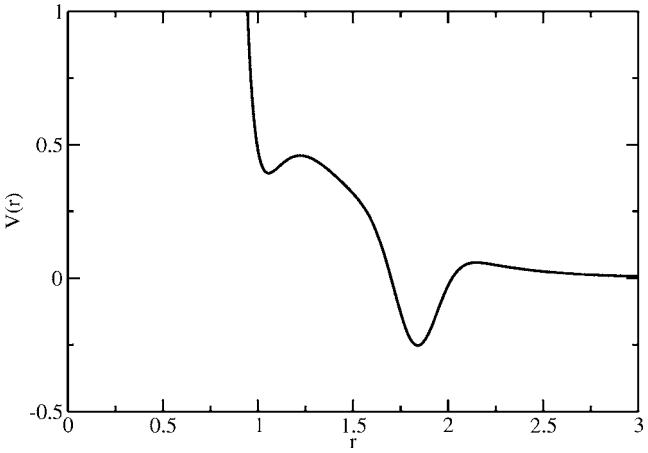

FIG. 15. The near-melting optimized honeycomb-lattice potential V_{HON}, as specified by Eq. (10).

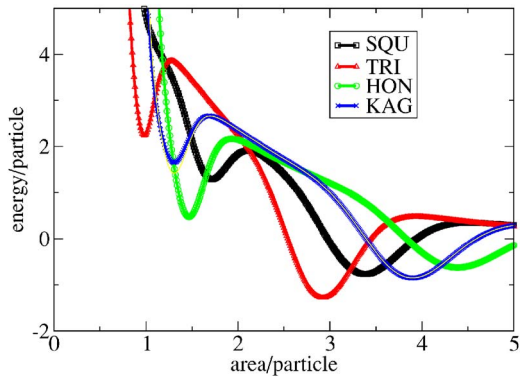

FIG. 16. (Color online) Lattice sums for the optimized honeycomb-lattice potential V_{HON}, as specified in Eq. (10). The honeycomb lattice is the most stable structure for values of α between 1.45 and 1.48.

structed pair interaction a weak long-ranged attractive component (Kac-Uhlenbeck-Hemmer potential [27]); the corresponding influence on the lattice sums is to subtract a contribution proportional to the number density, thus lowering the corresponding lattice sum toward a positive pressure regime. As they are, the lattice sums give a range of stability in pressure of 1.2 through 3.8, and in specific area of 1.42 through 1.48.

The 500-particle annealed MC simulation for this potential is shown in Fig. 18. The structure factor $S(\mathbf{k})$ for this configuration is shown in Fig. 19, and it indicates the presence of long-range order. Self-assembly has been achieved—although there are clearly defects, these were simply "frozen in" during annealing. Their presence *costs energy*, indicating that the defective structure is not the true ground state, as expected. The zero temperature scheme produced the potential

$$V_{\mathrm{HON}}(r) = \frac{5}{r^{12}} - \frac{6.50}{r^{10}} + 18.19\exp[-2.21r] - 0.4\exp[-40(r - 1.755)^2]. \quad (11)$$

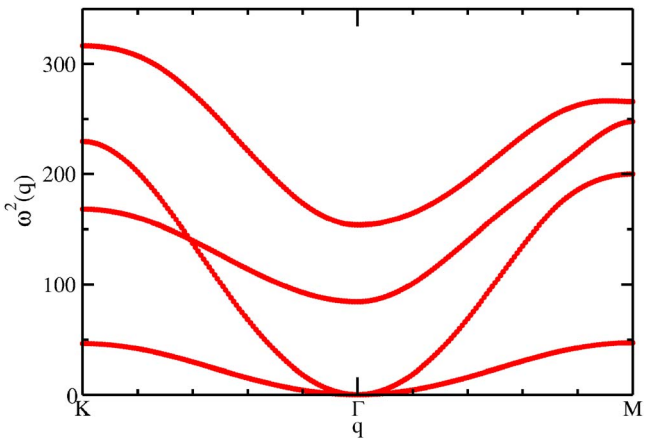

FIG. 17. (Color online) Phonon spectrum (frequency squared) for the optimized honeycomb-lattice potential V_{HON}, as specified by Eq. (10), at $\alpha=1.45$. Clearly the honeycomb lattice is mechanically stable.

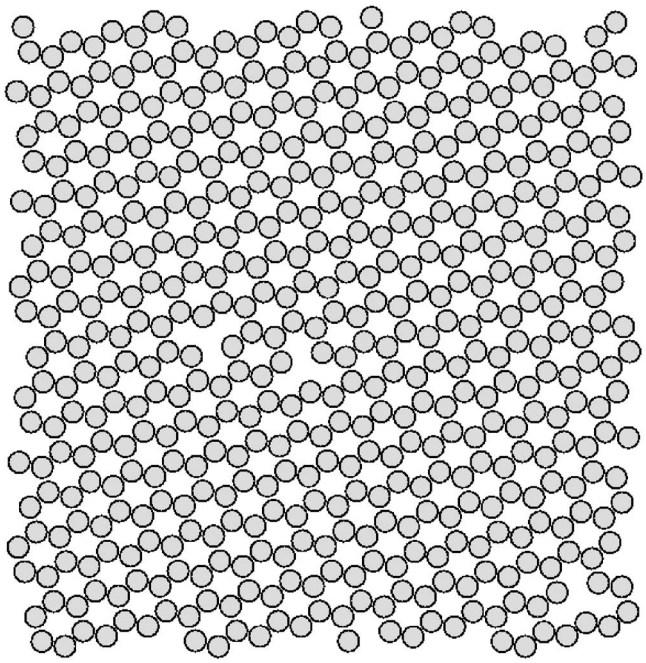

FIG. 18. 500-particle MC results annealed from $k_BT=0.22$ to $k_BT=0.0$ at $\alpha=1.45$ for the potential in Fig. 15.

Similarly to the square lattice, the zero-temperature scheme produced a honeycomb structure with long-range order, albeit with more defects [11 vacancies and 2 interstitials, compared to 3 vacancies and 0 interstitials for the function given in Eq. (10)].

VII. CONCLUSIONS AND DISCUSSION

In sum, we have introduced and demonstrated two optimization schemes for lattice self-assembly in two dimensions, each producing optimized pair potentials for the square and honeycomb lattices. The schemes are directly generalizable to three dimensions and to more complicated structures. Future work will do exactly this, testing whether schemes that work well for single component systems in two dimensions have wider applicability.

Although we have found potentials that have as their ground states the honeycomb and square lattices at particular

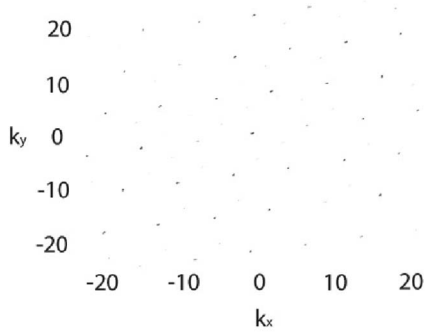

FIG. 19. $S(\mathbf{k})$ for configuration given in Fig. 18. Bragg spots shown here in $S(\mathbf{k})$ clearly indicate the presence of long-range order in the configuration shown in Fig. 18.

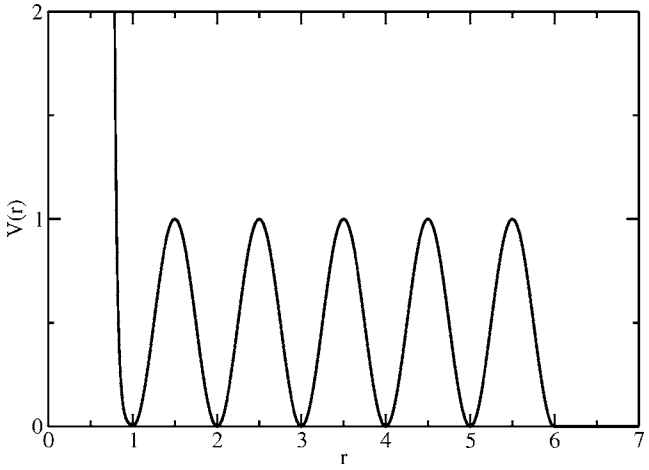

FIG. 20. Five-finger potential. Local minima are set at integer values to prevent local triangular or square structure from emerging.

α's, these functional forms for $V(r)$ are by no means unique. In future work, we will try to optimize for "robustness" in self-assembly. In particular, we would like to find potentials that not only cause self-assembly of a system of particles into a desired target structure, but that make the structure minimally sensitive to perturbations in density, pressure, and chemical potential, as well as to small changes in functional form of $V(r)$. This is extremely important if these potentials are to be implemented experimentally for two reasons. The first is that there is of course some experimental error in tuning the parameters in the potential, and these small uncertainties should not prevent self-assembly. The second is that we may wish to use experimental interactions to approximate optimal solutions with different parametrizations, and there will be some error associated with this fit. The potentials for the square and honeycomb lattices found in this work can indeed be called robust. For the square lattice potential, there is a wide range of parameter values around our optimal solutions that yield favorable lattice sums, real phonon frequencies, and produce near defect-free self-assembly. The important features of this potential are a strong initial repulsion (representing a near hard-core interaction), an attractive well at distance $\sqrt{\alpha}$ as well as a positive maximum (we used a gaussian) at or around $\sqrt{3\alpha}$. Not any functional form with these features will necessarily work; but we have found that perturbations around the potentials given above [relations (7) and (8)] that preserve these features do indeed cause square lattice self-assembly. The same can be said of the potentials derived for the honeycomb lattice [relations (10) and (11)], except of course with different features. These features are the strong initial repulsion, the positivity of the first minimum and the negativity of a second minimum, where the minima are at distance ratio $\sim\sqrt{3}$. The chosen α puts the first minimum at, or near, the honeycomb nearest neighbor.

It is a natural question to ask whether available colloidal interactions can be made to fit our optimized $V(r)$'s. Although obviously they cannot match these functions exactly, they can indeed form a good approximation. For example, our optimized honeycomb potential has a strong initial repulsion, followed by a short attraction, a steep repulsion and then another attraction. By adjusting relative amplitudes, this functional form can be approximated by a hard-core, a dispersion interaction, a repulsive dipole-dipole interaction, and an attractive depletion. There is indeed hope for using realizable interactions to form open structures in 2D colloidal systems.

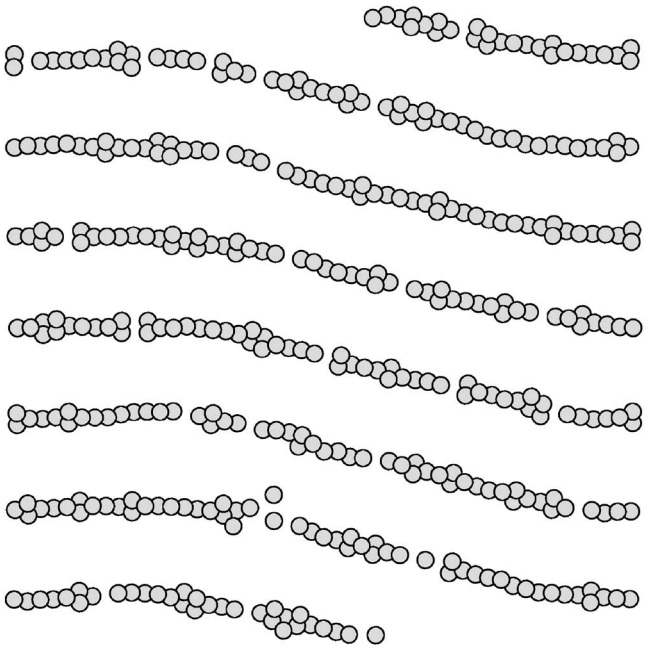

FIG. 21. 384-particle MC results for five-finger potential annealed to $k_BT=0.1$.

Extensive attempts were made to find a potential that stabilizes the Kagomé lattice but none were thoroughly successful. A potential was found that satisfied the necessary conditions, and the optimization was run. Although the MC run gave a lattice with long-range order, the interstitials were somewhat randomly placed. This is because there exists another 2D lattice with four coordination (as the Kagomé has) [28], and it and the Kagomé are nearly indistinguishible in energy for almost any LJ-based potential we used. Because of this closeness in energy, the interstitial sites themselves formed a weakly interacting lattice gas.

The problem of Kagomé lattice self-assembly goes beyond the competition with one other lattice, however. The Kagomé has the property that it is in many ways an intermediate between the triangular and honeycomb lattices: its density is in between the two; the first three coordination numbers are (4,6,4) as opposed to (6,6,6) in the triangular and (3,6,3) in the honeycomb lattice. So if the potential is significant for only the first three neighbors (as ours have been) then, rigorously, the Kagomé cannot energetically beat the honeycomb and triangular lattices over all densities. Furthermore, there is an extremely delicate energetic balance between a stable Kagomé and a phase separation into the triangular and honeycomb lattices. We believe that for these reasons our optimizations have been unable to cause self-assembly of the Kagomé.

The defects that were observed in the self-assembled triangular and honeycomb lattice do not disturb the crystal structure; this is to say that particles could be simply inserted

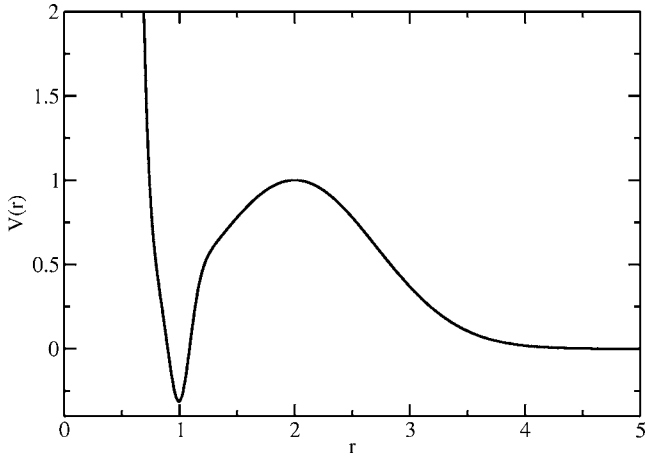

FIG. 22. Simplex potential. Attractive minimum followed by a sharp hump has the effect of favoring near neighbors while preventing second and third neighbors. This gives rise to the simplex clusters.

at the defect points and a perfect lattice would emerge. There are two possible reasons for the defects: first, that to have some number of them is energetically favorable, and thus the ground state configuration is not the perfect lattice; second, that the slow dynamics of the MC simulation at low temperatures prevent the defects from being removed in a realistic amount of CPU time. A look at the energetics shows that the second explanation is the right one. Over a small range of α around the simulation density, the perfect lattice has lower energy than that of the structure obtained in the simulation. Perhaps simulations in the μVT ensemble (grand canonical) would allow for more general phase space sampling and thus demonstrate that the gaps are spontaneously filled.

If it is possible to stabilize structures that were once thought to require directional bonding, what else can be stabilized? Bilayers? Block copolymers? For the purpose of seeing how far isotropic potentials can be taken, we examined what we call the "five-finger potential," shown in Fig. 20. We chose this form for the potential since it would inhibit second nearest neighbors of any lattice to form, only allowing long chains of particles. Annealed MC results for this are shown in Fig. 21. As shown, this potential allows for the assembly of such parallel chains at $\alpha=6.0$. This potential cannot be built in the lab with current technology—it is far too complex, but it shows that isotropic potentials have perhaps more flexibility than one would immediately think. It is also possible that a much simpler potential could allow for a similar structure to assemble.

We have also devised a circularly symmetric potential function that favors the assembly of small clusters of particles. The form of the potential was chosen to inhibit the formation of clusters with second and third (and so on) nearest neighbors—the most favorable structure thus being a *simplex*, or equilateral-triangle cluster. The structures we find are similar to those observed experimentally by Manoharan *et al.* [4]. Although they do not find the functional form of the potential explicitly, they conclude that the clusters that they observe cannot be a result only of van der Waals attraction and the hard core repulsion of the polystyrene colloid particles used in their experiment. This potential is shown in Fig. 22, which we run at specific area $\alpha=9.6$. MC results are shown in Fig. 23.

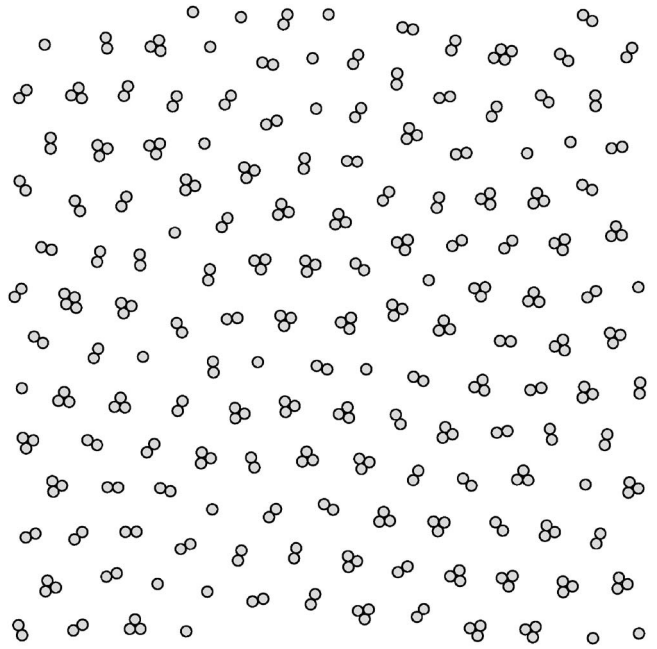

FIG. 23. 351-particle MC results for simplex potential annealed to $k_BT=0.1$.

One can imagine carrying on the process of qualitatively searching for isotropic potentials for more and more complex structures *ad infinitum*, with arbitrarily complex structures requiring more and more elaborate functional forms. For example, one might try to assemble a fullerene with a spherically symmetric pair potential by running an *NVT* annealing simulation with 60 particles interacting via a potential that has sharp minima at every interparticle distance for that molecule. There must be a limit, however: although it is conceivable that a chiral structure would self-assemble, we cannot choose its chirality if we employ only an isotropic potential (left and right handed structures are equally likely). A key question that we ask, and that this study answers only in part, is whether we can make qualitative statements about the types of structures that can be assembled using only isotropic pair interactions.

We are currently working on expanding this work to three dimensional systems. Moreover, we are exploring the possibility of tailoring for self-assembly thermodynamic quantities besides the area or volume, such as the pressure (in an *NPT* ensemble simulation) and the chemical potential (in a μVT ensemble simulation). In future work, we plan to explore the self-assembly properties of multicomponent media using our inverse/optimization approach.

ACKNOWLEDGMENT

This work was supported by the Office of Basic Energy Sciences, DOE, under Grant No. DE-FG02-04ER46108.

[1] G. M. Whitesides and B. Grzybowski, Science **295**, 2418 (2002).
[2] S. A. Jenekhe and X. L. Chen, Science **283**, 372 (1999).
[3] A. M. Jackson, J. W. Myerson, and F. Stellacci, Nat. Mater. **3**, 330 (2004).
[4] V. N. Manoharan, M. T. Elsesser, and D. J. Pine, Science **301**, 483 (2003).
[5] E. A. Jagla, Phys. Rev. E **58**, 1478 (1998).
[6] P. Ziherl and R. Kamien, e-print cond-mat/0103171.
[7] K. M. Ho, C. T. Chan, and C. M. Soukoulis, Phys. Rev. Lett. **65**, 3152 (1990).
[8] O. Sigmund and S. Torquato, Appl. Phys. Lett. **69**, 3203 (1996).
[9] T. A. Mary, J. S. O. Evans, T. Vogt, and A. W. Sleight, Science **272**, 90 (1996).
[10] B. Xu, F. Arias, S. T. Britain, X.-M. Zhao, B. Gryzbowski, S. Torquato, and G. M. Whitesides, Adv. Mater. (Weinheim, Ger.) **11**, 1186 (1999).
[11] S. Hyun and S. Torquato, J. Mater. Res. **16**, 280 (2001).
[12] G. Ferey and A. Cheetham, Science **283**, 1125 (1999).
[13] B. Chen, M. Eddaoudi, S. Hyde, M. O'Keeffe, and O. Yaghi, Science **291**, 1021 (2001).
[14] A. L. Greer, Nature (London) **404**, 134 (2000).
[15] C. A. Murray and D. G. Grier, Annu. Rev. Phys. Chem. **47**, 421 (1996).
[16] Z. L. Zhang, M. A. Horsch, M. H. Lamm, and S. C. Glotzer, Nano Lett. **3**, 1341 (2004).
[17] M. Watzlawek, C. N. Likos, and H. Lowen, Phys. Rev. Lett. **82**, 5289 (1999).
[18] M. Rechtsman, F. H. Stillinger, and S. Torquato, Phys. Rev. Lett. **95**, 228301 (2005).
[19] T. A. Weber and F. H. Stillinger, Phys. Rev. E **48**, 4351 (1993).
[20] A. P. Lyubartsev and A. Laaksonen, Phys. Rev. E **52**, 3730 (1995).
[21] H. Meyer, O. Biermann, R. Faller, D. Reith, and F. Muller-Plathe, J. Chem. Phys. **113**, 6264 (2000).
[22] N. Ashcroft and N. D. Mermin, *Solid State Physics* (Holt, Rinehart, and Winston, New York, 1964).
[23] T. V. Ramakrishnan and M. Yussouff, Phys. Rev. B **19**, 2775 (1979).
[24] D. Chandler, Science **220**, 787 (1983).
[25] P. J. Camp, Phys. Rev. E **68**, 061506 (2003).
[26] A. Quandt and M. P. Teter, Phys. Rev. B **59**, 8586 (1999).
[27] M. Kac, G. Uhlenbeck, and P. Hemmer, J. Math. Phys. **4**, 216 (1962).
[28] S. Torquato and F. H. Stillinger, J. Phys. Chem. B **105**, 11849 (2001).